Spirobifluorene-Linked Bisanthracene: An Efficient Blue Emitter with Pronounced Thermal Stability

Wen-Jian Shen,[†] Rajasekhar Dodda,[†] Chang-Ching Wu,[†] Fang-Iy Wu,[†] Tswen-Hsin Liu,[†] Hsian-Hung Chen,[†] Chin H. Chen,[‡] and Ching-Fong Shu*[,†]

Department of Applied Chemistry and Microelectronics and Information Systems Research Center, National Chiao Tung University, Hsin-Chu, Taiwan 300, Republic of China

Received June 19, 2003. Revised Manuscript Received December 28, 2003

Spiro-**FPA**, a novel blue emitter, in which two identical anthracene luminophores are linked orthogonally around a spirobifluorene core, has been synthesized and characterized. The introduction of a spiro linkage into the structure of spiro-**FPA** leads to a reduction in crystallization tendency and an increase in glass transition temperature relative to the monomeric units. In addition, the tetrahedral nature of the carbon atom at the spiro center preserves the optical and electrochemical characteristics of the pristine anthracene units. As demonstrated by AFM measurements, high-quality amorphous films of spiro-**FPA** with good morphological stability can be prepared by vapor deposition. Organic EL devices constructed using a 1.0-wt % **TBP**-doped spiro-**FPA** emitting layer produce bright blue emissions with a high luminescence efficiency of 4.9 cd/A (2.07 lm/W).

Introduction

Since the discovery of multilayered organic light-emitting diodes (OLEDs) by Tang et al.,[1] electroluminescent devices have been the subject of intensive investigation because of their applications in full-color displays.[2] Recently, various studies have been focused on improving the durability of OLEDs. The tendency of small molecules to crystallize spontaneously upon exposure to heat presents a limitation for LED applications, as crystal formation destroys film homogeneity and crystal boundaries raise the resistance of the sample, eventually leading to electrical shorting.[3] A considerable amount of evidence indicates that an amorphous thin film (in OLEDs) with a high glass transition temperature (T_g) is less vulnerable to heat and, hence, the device performance is more stable.[4] Different synthetic approaches have been pursued to confer a higher stability to the glass state of low-molecular-weight compounds. Several distinct classes of glass-forming small molecules with elevated values of T_g have been synthesized, including spiro-shaped, "starburst", dendritic, tetrahedral, and cardo molecules.[5−9] Salbeck et al. have synthesized spiro-type molecules based on 9,9′-spirobifluorene,[4b,5a−c] which consists of two identically substituted-fluorene moieties connected through an sp^3-hybridized carbon atom: the spiro center. In the spiro segment, the rings of the connected bifluorene entities are arranged orthogonally.[10] This structural feature not only hinders close packing and intermolecular interactions, but also increases the molecular rigidity. As a result, the introduction of a spirobifluorene linkage into the structure of small molecules leads to a reduction in

* To whom correspondence should be addressed. E-mail: shu@cc.nctu.edu.tw.

[†] Department of Applied Chemistry.

[‡] Microelectronics and Information Systems Research Center.

(1) Tang, C. W.; Van Slyke, S. A. *Appl. Phys. Lett.* **1987**, *51*, 913.

(2) (a) *Organic Electroluminescent Materials and Devices*; Miyata, S., Nalwa, H. S., Eds.; Cordon and Breach: New York, 1997. (b) Chen, C. H.; Shi, J.; Tang, C. W. *Macromol. Symp.* **1997**, *125*, 1. (c) Chen, C. H.; Shi, J.; Tang, C. W. *Coord. Chem. Rev.* **1998**, *171*, 161. (d) Mitschke, U.; Bäuerle, P. *J. Mater. Chem.* **2000**, *10*, 1471. (e) Hung, L. S.; Chen, C. H. *Mater. Sci. Eng., R* **2002**, *39*, 143.

(3) Joswick, M. D.; Cambell, I. H.; Barashkov, N. N.; Ferraris, J. P. *J. Appl. Phys.* **1996**, *80*, 2883.

(4) (a) Tokito, S.; Tanaka, H.; Noda, K.; Okada, A.; Taga, Y. *Appl. Phys. Lett.* **1997**, *70*, 1929. (b) Salbeck, J.; Yu, N.; Bauer, J.; Weissörtel, F.; Bestgen, H. *Synth. Met.* **1997**, *91*, 209. (c) Konne, B. E.; Loy, D. E.; Thompson, M. E. *Chem. Mater.* **1998**, *10*, 2235. (d) O'Brien, D. F.; Burrows, P. E.; Forrest, S. R.; Konne, B. E.; Loy, D. E.; Thompson, M. E. *Adv. Mater.* **1998**, *10*, 1108. (e) Steuber, F.; Staudigel, J.; Stössel, M.; Simmerer, J.; Winnacker, A.; Spreitzer, H.; Weissörtel, F.; Salbeck, J. *Adv. Mater.* **2000**, *12*, 130. (f) Shirota, Y. *J. Mater. Chem.* **2000**, *10*, 1.

(5) (a) Salbeck, J.; Bauer, J.; Weissörtel, F. *Macromol. Symp.* **1997**, *125*, 121. (b) Johansson, N.; dos Santos, D. A.; Guo, S.; Cornil, J.; Fahlman, M.; Salbeck, J.; Schenk, H.; Arwin, H.; Brédas, J. L.; Salenek, W. R. *J. Chem. Phys.* **1997**, *107*, 2542. (c) Johansson, N.; Salbeck, J.; Bauer, J.; Weissörtel, F.; Bröms, P.; Andersson, A.; Salaneck, W. R. *Adv. Mater.* **1998**, *10*, 1136. (d) Kim, Y. H.; Shin, D. C.; Kim, S. H.; Ko, C. H.; Yu, H. S.; Chae, Y. S.; Kwon, S. K. *Adv. Mater.* **2001**, *13*, 1690. (e) Wu, C. C.; Lin, Y. T.; Chiang, H. H.; Cho, T. Y.; Chen, C. W.; Wong, K. T.; Liao, Y. L.; Lee, G. H.; Peng, S. M. *Appl. Phys. Lett.* **2002**, *81*, 577.

(6) (a) Inada, H.; Shirota, Y. *J. Mater. Chem.* **1993**, *3*, 319. (b) Ueta, E.; Nakano, H.; Shirota, Y. *Chem. Lett.* **1994**, 2397. (c) Kageyama, H.; Itano, K.; Ishikawa, W.; Shirota, Y. *J. Mater. Chem.* **1996**, *6*, 675. (d) Thelakkat, M.; Schmidt, H. *Adv. Mater.* **1998**, *10*, 219. (e) Wu, I. Y.; Lin, J. T.; Tao, Y. T.; Balasubramaniam, E.; Su, Y. Z.; Ko, C. W. *Chem. Mater.* **2001**, *13*, 2626.

(7) (a) Bettenhausen, J.; Strohriegl, P. *Adv. Mater.* **1996**, *8*, 507. (b) Bettenhausen, J.; Greczmiel, M.; Jandke, M.; Strohriegl, P. *Synth. Met.* **1997**, *91*, 223. (c) Tanaka, S.; Iso, T.; Doke, Y. *Chem. Commun.* **1997**, 2063. (d) Meier, H.; Lehmann, M. *Angew. Chem., Int. Ed.* **1998**, *37*, 643. (e) Sakamoto, Y.; Suzuki, T.; Miura, A.; Fujikawa, H.; Tokito, S.; Taga, Y. *J. Am. Chem. Soc.* **2000**, *122*, 1832.

(8) (a) Robinson, M. R.; Wang, S.; Bazan, G. C.; Cao, Y. *Adv. Mater.* **2000**, *12*, 1701. (b) Wang, S.; Oldham, W. J., Jr.; Hudack, R. A., Jr.; Bazan, G. C. *J. Am. Chem. Soc.* **2000**, *122*, 5695. (c) Chan, L. H.; Yeh, H. C.; Chen, C. T. *Adv. Mater.* **2001**, *13*, 1637. (d) Yeh, H. C.; Lee, R. H.; Chan, L. H.; Lin, Y. J.; Chen, C. T.; Balasubramaniam, E.; Tao, Y. T. *Chem. Mater.* **2001**, *13*, 2788.

(9) (a) Wong, K. T.; Wang, Z. J.; Chien, Y. Y.; Wang, C. L. *Org. Lett.* **2001**, *3*, 2285. (b) Ko, C. W.; Tao, Y. T. *Synth. Met.* **2002**, *126*, 37.

(10) Wu, R.; Schumm, J. S.; Pearson, D. L.; Tour, J. M. *J. Org. Chem.* **1996**, *61*, 6906.

10.1021/cm0345117 CCC: $27.50
Published on Web 01/30/2004

the tendency to crystallize, an enhancement in solubility, and an increase in glass transition temperature. In addition, the tetrahedral nature of the carbon atom at the spiro center connects the conjugated moieties through a σ-bonded network, which in turn serves as a conjugation interrupt, and, thus, most of the desired electronic and optical properties of the corresponding nonspiro molecules are preserved.[11]

Organic light-emitting materials with large band gap energies that emit blue light efficiently are of special interest, because they are desired for use as blue light sources in full-color display applications and also because they can serve as energy-transfer donors in the presence of lower-energy fluorophores.[12] Among the blue fluorescent materials, 9,10-diphenylanthracene (**DPA**), which has near unity fluorescence quantum efficiency in solution,[13] is attractive, but it has the inherent problem of crystallizing when deposited as a thin film in a device.[14] To avoid the formation of polycrystalline films and to improve its thermal properties, our aim was to introduce the 9,9′-spirobifluorene linkage into **DPA** without altering its photophysical characteristics. Herein, we report the synthesis and characterization of a high-T_g and efficient blue-emitting material, 2,2′-bis(10-phenylanthracen-9-yl)-9,9′-spirobifluorene (spiro-**FPA**), in which the two identical luminophores are aligned orthogonally through bonding to an sp^3-hybridized carbon atom: a spiro center. Additionally, we report the fabrication and performance of blue-emitting OLEDs using spiro-**FPA** as the emitter itself or as a host emitting material doped with 2,5,8,11-tetra-*tert*-butylperylene (**TBP**).[15]

Experimental Section

General Directions. Compound **1** was synthesized as described in a literature procedure.[16] The solvents were dried using standard procedures. All other reagents were used as received from commercial sources, unless otherwise stated. Differential scanning calorimetry was performed on a SEIKO DSC 6200 unit using a heating rate of 20 °C min^{-1} and a cooling rate of 50 °C min^{-1}. TGA was undertaken on a Perkin-Elmer Pyris 1 TGA instrument with a heating rate of 10 °C min^{-1}. UV−Visible spectra were measured with an HP 8453 diode array spectrophotometer. PL spectra were obtained on a Hitachi F-4500 luminescence spectrometer. Cyclic voltammetry measurements were performed on a BAS 100 B/W electrochemical analyzer with 0.1 M tetrabutylammonium hexafluorophosphate ($TBAPF_6$) as the supporting electrolyte. EL devices were fabricated under a base vacuum of 10^{-6} Torr in a thin-film evaporation coater and characterized following a published protocol.[17] AFM pictures were recorded with a Digital Instruments Nanoscope E scanning probe microscope.

Scheme 1. Synthesis of Spirobifluroene-Linked Spiro-FPA

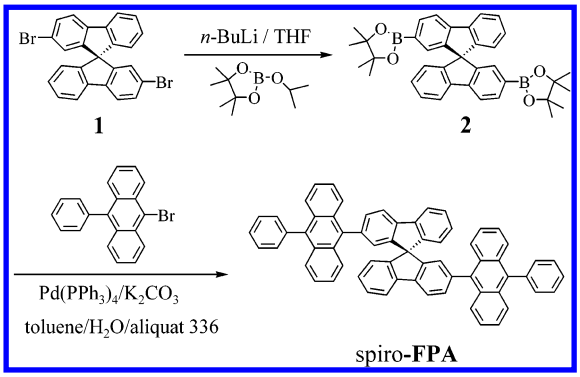

2,2′-Bis(4,4,5,5-tetramethyl-1,3,2-dioxaborolane-2-yl)-9,9′-spirobifluorene (2). *n*-Butyllithium (8.8 mL, 22.0 mmol, 2.5 M solution in hexane) was added at −78 °C under N_2 to a solution of 2,2′-dibromo-9,9′-spirobifluorene (**1**, 3.0 g, 6.3 mmol) in dry THF (20 mL). After the addition was complete, the reaction mixture was warmed to 0 °C for 15 min and then cooled to −78 °C. 2-Isopropoxy-4,4,5,5-tetramethyl-1,3,2-dioxaborolane (3.2 mL, 15.8 mmol) was rapidly added to the mixture with constant stirring. The solution was warmed slowly to room temperature and then stirred for 12 h. The reaction mixture was quenched with H_2O and extracted with Et_2O. The organic extracts were washed successively with brine and H_2O, and then dried ($MgSO_4$). Concentration of the Et_2O solution, followed by recrystallization with hexane/CH_2Cl_2, afforded **2** (1.43 g, 40%). ^1H NMR (300 MHz, $CDCl_3$): δ 7.83−7.85 (m, 6H), 7.33 (ddd, J = 7.5, 7.5, 0.9 Hz, 2H), 7.15 (d, J = 1.2 Hz, 2H), 7.07 (ddd, J = 7.5, 7.5, 0.9 Hz, 2H), 6.64 (d, J = 7.6 Hz, 2H), 1.24 (s, 24H). ^{13}C NMR (75 MHz, $CDCl_3$): δ 149.6, 147.6, 145.1, 141.5, 134.8, 130.5, 128.3, 127.6, 124.1, 120.5, 119.4, 83.7, 66.0, 24.9. HRMS-EI (m/z): [M^+] calcd. for $C_{37}H_{38}B_2O_4$, 568.2956; found, 568.2953.

2,2′-Bis(10-phenylanthracene-9-yl)-9,9′-spirobifluorene (3). Aqueous K_2CO_3 (2.0 M, 3.0 mL) and Aliquat 336 (80 mg) were added to a solution of 9-bromo-10-phenylanthracene (1.58 g, 4.75 mmol) and **2** (1.00 g, 1.76 mmol) in toluene (20.0 mL). The mixture was degassed and tetrakis(triphenylphosphine)palladium (80 mg, 3.9 mol %) was added in one portion under an atmosphere of N_2. The solution was then heated under reflux for 24 h under N_2. After the solution cooled, the solvent was evaporated under vacuum and the product was extracted with $CHCl_3$. The $CHCl_3$ solution was washed with brine and H_2O, and then dried ($MgSO_4$). Evaporation of the solvent, followed by recrystallization from $CHCl_3$/EtOAc, afforded **3** (1.1 g, 76%). ^1H NMR (300 MHz, $CDCl_3$): δ 7.99 (d, J = 7.5 Hz, 2H), 7.88 (d, J = 7.5 Hz, 2H), 7.56−7.69 (m, 14H), 7.39−7.48 (m, 8H), 7.26−7.30 (m, 6H), 7.24 (ddd, J = 7.5, 7.5, 0.9 Hz, 2H), 7.02−7.09 (m, 6H). ^{13}C NMR (75 MHz, $CDCl_3$): δ 149.4, 149.1, 141.7, 141.2, 139.1, 138.6, 137.1, 131.3, 131.0, 129.9, 129.8, 128.5, 128.4, 128.1, 128.0, 127.5, 127.2, 127.0, 126.9, 126.8, 125.4, 125.1, 125.0, 124.2, 120.2, 120.0, 66.2. HRMS−FAB (m/z): [M^+] calcd. for $C_{65}H_{40}$, 820.3130; found, 820.3130.

Results and Discussion

Synthesis. Scheme 1 illustrates the synthetic route for the preparation of the bis(phenylanthracene) derivative containing a spirobifluorene skeleton. The dibromide **1** was synthesized by direct bromination of 9,9′-spirobifluorene as described in a literature procedure.[16] The lithiation of **1** with an excess of *n*-BuLi, followed by treatment with 2-isopropoxy-4,4,5,5-tetramethyl-1,3,2-dioxaborolane, gave the bis(boronic ester) **2**. The Pd-catalyzed Suzuki coupling reaction between the

(11) (a) Chiang, C. L.; Shu, C. F. *Chem. Mater.* **2002**, *14*, 682. (b) Wu, F. I.; Dodda, R.; Reddy, D. S.; Shu, C. F. *J. Mater. Chem.* **2002**, *12*, 2893.

(12) (a) Kido, J.; Hongawa, K.; Okuyama, K.; Nagai, K. *Appl. Phys. Lett.* **1994**, *64*, 815. (b) Kido, J.; Shionoya, H.; Nagai, K. *Appl. Phys. Lett.* **1995**, *67*, 2281. (c) Chen, F. C.; Yang, Y.; Thompson, M. E.; Kido, J. *Appl. Phys. Lett.* **2002**, *80*, 2308.

(13) Berlan, I. B. *Handbook of Fluorescence Spectra of Aromatic Molecules*, 2nd ed.; Academic Press: New York, 1971.

(14) Adachi, C.; Tsutsui, T.; Saito, S. *Appl. Phys. Lett.* **1990**, *56*, 799.

(15) (a) Mi, B. X.; Gao, Z. Q.; Lee, C. S.; Lee, S. T.; Kwong, H. L.; Wang, N. B. *Appl. Phys. Lett.* **1999**, *75*, 4055. (b) Shi, J.; Tang, C. W. *Appl. Phys. Lett.* **2002**, *80*, 3201.

(16) Pei, J.; Ni, J.; Zhou, X. H.; Cao, X. Y.; Lai, Y. H. *J. Org. Chem.* **2002**, *67*, 4924.

(17) Chen, C. H.; Tang, C. W. *Appl. Phys. Lett.* **2001**, *79*, 3711.

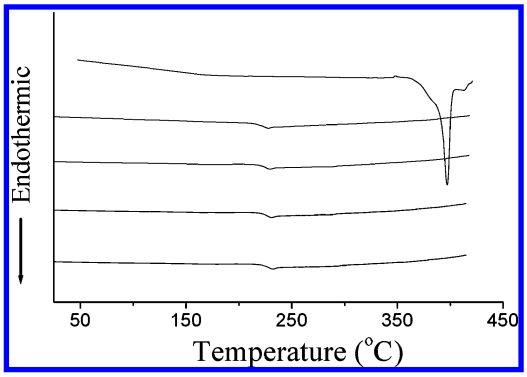

Figure 1. DSC thermograms of spiro-**FPA** with sequential heating and cooling cycles (first to fifth heatings are represented from top to bottom).

bisboronate **2** and 9-bromo-10-phenylanthracene[18] afforded the spirobifluorene-linked bis(phenylanthracene), spiro-**FPA**.[19] The structures of compound **2** and spiro-**FPA** were verified by ^{1}H and ^{13}C NMR spectroscopy, as well as by mass spectrometry.

Thermal Properties. The thermal properties of the spiro-linked anthracene derivative were investigated by differential scanning calorimetry (DSC) and thermogravimetric analysis (TGA). DSC was performed in the temperature range from 30 to 430 °C. Figure 1 displays the DSC curves of a sample recrystallized from chloroform/ethyl acetate. The sample melts at 397 °C on the first heating only, and then it changes into a glassy state upon cooling from the melt. When the amorphous glassy sample is heated again, a glass transition occurs at 223 °C and no exothermic peak due to crystallization is observed up to 430 °C. On subsequent cooling and heating cycles, just the glass transition phenomenon remains in the DSC thermogram, i.e., without recrystallization. This observation indicates the prominent stability of the amorphous glass state of this material, which can be attributed to the presence of the spiro-fused orthogonal bifluorene linkage. Spiro-**FPA** also exhibits a high thermochemical stability, as evidenced by thermogravimetric analysis, with its 5%-weight-loss temperatures under nitrogen atmosphere being up to 450 °C.

To investigate the morphological stability of a spiro-**FPA** film, we prepared a thin film on an indium tin oxide (ITO) substrate by vapor deposition and measured its surface morphology by atomic force microscopy (AFM) before and after annealing at 95 °C for 3 d under a nitrogen atmosphere.[20] As indicated by Figure 2a, the thin layer of spiro-**FPA** displayed a fairly good surface morphology that did not change upon annealing. For comparison, the same experiments were conducted with a film of 9,10-di-(2-naphthyl)anthracene (**DNA**), which is a prototypical host material for blue-emitting electroluminescent devices.[15b,21] Upon deposition, the surface was quite rough and many small crystals were observed on the **DNA** layer. As Figure 2b indicates, the annealing induced a further degradation of the surface morphology and, in addition, large crystals were observed on the annealed layer. It is evident that the thermal stability of spiro-**FPA** is an improvement over that of **DNA**, presumably because the presence of the spiro linkage depresses the ability of spiro-**FPA** to crystallize, and so it maintains its morphological stability in the glassy state.

Photophysical Properties. Figure 3 depicts the absorption and photoluminescence (PL) spectra of spiro-**FPA** in dilute solution and in the solid state. The absorption spectrum in toluene solution exhibits the characteristic vibrational pattern of the isolated anthracene group. Upon excitation, the solution shows a blue PL with an emission maximum at 425 nm. The PL spectrum is comparable with that obtained from **DPA** in toluene (not depicted in Figure 3) and has a 14-nm red-shift, which is probably due to the increase of the conjugation of spiro-**FPA** relative to **DPA** after the phenyl ring has been replaced by the fluorene ring. This observation suggests that the quarternary carbon atom at the spiro center serves as a conjugation interrupt, with the effect of retaining the desired optical properties of the nonappended parent molecule. The absorption and emission spectra of the spiro-**FPA** thin film, prepared by spin-coating from a toluene solution onto a quartz plate, are similar to those in dilute solution and exhibit red-shifts of 5 and 19 nm, respectively. The spectral shifts observed in the solid state probably are due to the difference in dielectric constant of the environment.[4b]

Electrochemistry. Figure 4 displays the electrochemical behavior of spiro-**FPA** when investigated by cyclic voltammetry using ferrocene as the internal standard. During the anodic scan in CH_2Cl_2, a reversible oxidation was observed at 0.76 V (E°′) with the onset potential at 0.67 V. Upon the cathodic sweep in THF, a reversible reduction was detected at −2.42 V (E°′) with the onset potential at −2.35 V. The reversible reductive and oxidative behavior indicates that the anthracene derivative can be utilized as a hole- and electron-transporter.[22] The HOMO and LUMO energy levels of spiro-**FPA** estimated from the onset potential of the p-doping and n-doping, respectively, are −5.47 and −2.45 eV with respect to the energy level of the ferrocene reference (4.8 eV below the vacuum level).[23] The band gap of spiro-**FPA** (3.02 eV) estimated from electrochemical measurements is in agreement with the result of the optical absorption threshold (2.97 eV). It is also worth mentioning that the spiro-linked anthracene moieties are noninteracting redox centers, as they are electrochemically equivalent and oxidize (and reduce) simultaneously at the same potential.[24] This observation is consistent with the notion that the sp^3-hybridized carbon atom at the spiro center effectively interrupts the conjugation.

(18) Zhang, X. M.; Bordwell, F. G.; Bares, J. E.; Cheng, J. P.; Petrie, B. C. *J. Org. Chem.* **1993**, *58*, 3051.
(19) Miyaura, N.; Suzuki, A. *Chem. Rev.* **1995**, *95*, 2457.
(20) (a) Han, E.; Do, L.; Niidome, Y.; Fujihira, M. *Chem. Lett.* **1994**, 969. (b) Smith, P. F.; Gerroir, P.; Xie, S.; Hor, A. M.; Popovic, Z.; Hair, M. L. *Langmuir* **1998**, *14*, 5946. (c) Choi, J.-W.; Kim, J. S.; Oh, S. Y.; Rhee, H.-W.; Lee, W. H.; Lee, S. B. *Thin Solid Films* **2000**, *363*, 271. (d) Mori, T.; Mitsuoka, T.; Ishii, M.; Fujikawa, H.; Taga, Y. *Appl. Phys. Lett.* **2002**, *80*, 3895.
(21) Li, C.-L.; Shieh, S.-J.; Lin, S.-C.; Liu, R.-S. *Org. Lett.* **2003**, *5*, 1131.
(22) Gu, J.; Kawabe, M.; Masuda, K.; Namba, S. *J. Appl. Phys.* **1977**, *48*, 2493.
(23) Pommerehne, J.; Vestweber, H.; Guss, W.; Mahrt, R. F.; Bässler, H.; Porsch, M.; Daub, J. *Adv. Mater.* **1995**, *7*, 551.
(24) (a) Flanagan, J. B.; Margel, S.; Bard, A. J.; Anson, F. A. *J. Am. Chem. Soc.* **1978**, *100*, 4248. (b) Shu, C. F.; Shen, H. M. *J. Mater. Chem.* **1997**, *7*, 47.

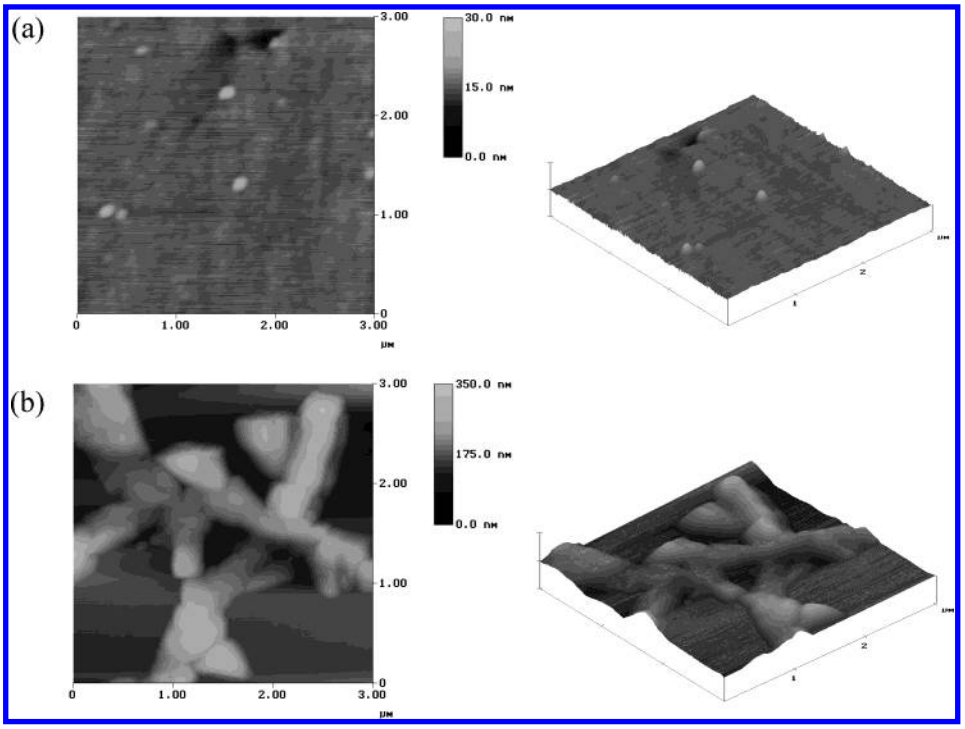

Figure 2. AFM images (top and angled views) of (a) a spiro-**FPA** layer and (b) a **DNA** layer, after annealing at 95 °C for 3 d under a nitrogen atmosphere.

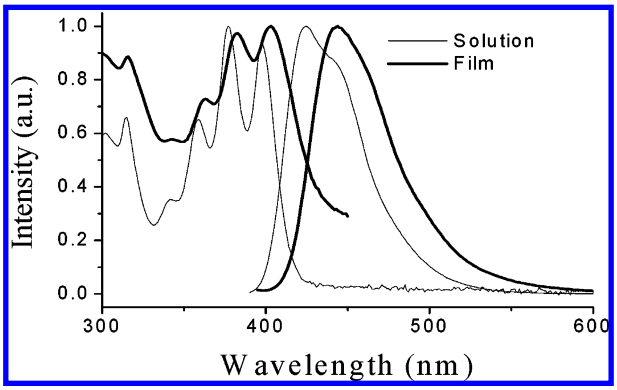

Figure 3. UV−Vis absorption and PL spectra of spiro-**FPA** in toluene solution and in the solid state.

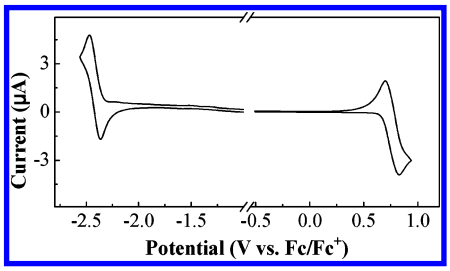

Figure 4. Cyclic voltammogram of spiro-**FPA**.

Electroluminescent Devices. To study the electroluminescence properties of spiro-**FPA**, we fabricated multilayer devices with the configuration of ITO/copper phthalocyanine (CuPc)/4,4′-bis[*N*-(1-naphthyl)-*N*-phenylamino]biphenyl (NPB)/spiro-**FPA**:*x*% **TBP**/Alq_3/LiF)/Al (150:400:200:200:10:2000 Å). In this structure, ITO and Al are the anode and cathode, respectively. The stack of organic layers consists of CuPc as the anode buffer layer, NPB as the hole-transport layer, spiro-**FPA**:*x*% **TBP** as the emitter, Alq_3 as the electron-transport layer, and LiF as the electron-injection layer. In this study, a nonplanar derivative of perylene, **TBP**, which is a prototypical dopant for blue-emitting electroluminescent devices,[15] was chosen as the dopant. The spiro-**FPA**-doped **TBP** emissive layer was produced by co-depositing spiro-**FPA** and **TBP** simultaneously. Reference devices that used **DNA**:*x*% **TBP** as the emitter were also constructed for the sake of comparison.

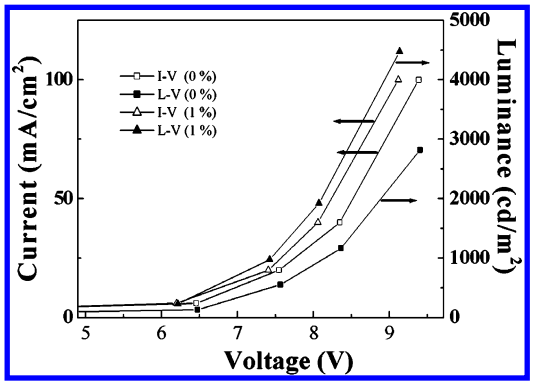

Figure 5. Current−voltage characteristics and luminescence−voltage characteristics of undoped and 1.0-wt %-**TBP**-doped spiro-**FPA** devices, having the configurations ITO/CuPc/NPB/spiro-**FPA**:*x*% **TBP**/Alq_3/LiF/Al.

The current−voltage−luminance (*I*−*V*−*L*) characteristics of the devices based on spiro-**FPA** are shown in Figure 5, and their performances are listed in Table 1. The EL emission spectra of undoped, and 1.0-wt %-**TBP**-doped, spiro-**FPA** cells are also depicted in Figure 6. In the undoped cell, the EL spectrum is featureless, with the maximum peak intensity at 460 nm. The similarity of the PL and EL spectra indicates that the EL is attributed to an emission from a singlet excited state of spiro-**FPA**. The device electroluminescent efficiency achieves 2.76 cd/A (corresponding to a power efficiency of 1.15 lm/W) at 20 mA/cm^2 and exhibits a better blue CIE chromaticity (x = 0.158, y = 0.141). At a dopant concentration of 0.5 wt %, the EL spectrum shows **TBP**

Table 1. EL Performance of Spiro-FPA-Based Devices[a,b]

doping concn. (wt %)	driving voltage (V)	current efficiency (cd/A)	power efficiency (lm/W)	C. I. E. coord. *x*, *y*
0.0	7.55 (9.39)	2.76 (2.82)	1.15 (0.94)	0.16, 0.14 (0.16, 0.14)
0.5	7.54 (9.26)	4.77 (4.40)	1.98 (1.49)	0.14, 0.20 (0.14, 0.20)
1.0	7.41 (9.12)	4.88 (4.47)	2.07 (1.54)	0.13, 0.21 (0.14, 0.20)
1.5	7.31 (9.12)	3.83 (3.75)	1.65 (1.29)	0.14, 0.22 (0.14, 0.22)
2.0	7.47 (9.28)	3.69 (3.59)	1.55 (1.21)	0.14, 0.23 (0.14, 0.22)
0.0[c]	6.48 (8.23)	1.86 (1.70)	0.90 (0.65)	0.18, 0.20 (0.17, 0.18)
1.0[c]	6.58 (8.13)	3.77 (3.27)	1.80 (1.26)	0.15, 0.24 (0.15, 0.23)

[a] Measured at 20 mA/cm^2. [b] The data in parentheses were taken at a current density of 100 mA/cm^2. [c] DNA-based devices.

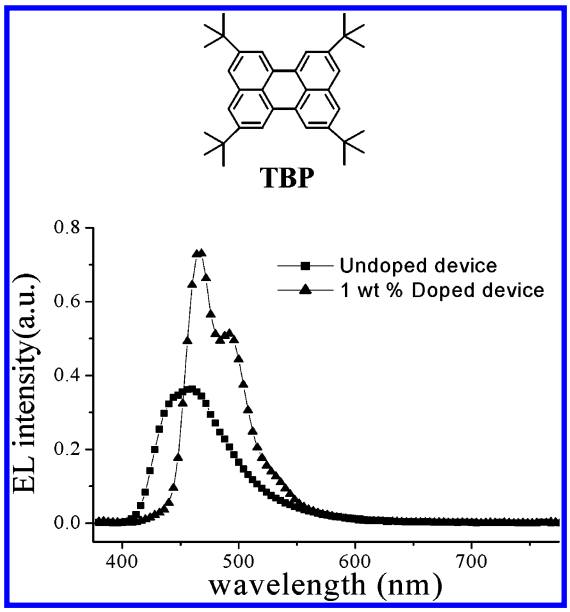

Figure 6. EL spectra of undoped and 1.0-wt %-**TBP**-doped spiro-**FPA** devices, and the chemical structure of **TBP**.

emission together with a contribution from the host emission of spiro-**FPA** that is due to the incomplete energy transfer. Increasing the doping level to 1.0 wt % results in a complete energy transfer. The emission spectrum shows only narrow vibronic features that are characteristic of the **TBP** dopant. The efficiency increases to 4.88 cd/A (corresponding to 2.07 lm/W), with a slight red-shift in the CIE coordinates ($x = 0.134$, $y = 0.207$). Raising the driving currents results merely in a slow falloff in EL efficiency and a slight shift in EL color. For the 1.0%-doped device, the efficiency is maintained near 4.47 cd/A up to 100 mA/cm^2 with color coordinates of (0.135, 0.202). We noted that the EL efficiency drops on going from a dopant concentration of 1.0 to 2.0%. This may be due to self-quenching of the dopant emission at higher concentration. The efficiency, however, remains greater than 3.0 cd/A. Table 1 also presents the EL data of the DNA-based devices. In addition to the improved morphological stability (vide supra), spiro-**FPA** exhibits superior EL performance over that of **DNA**, such as higher values of current- and power-efficiency and a more-saturated blue color.

In summary, we have synthesized a novel blue emitter, spiro-**FPA**, in which two identical anthracene luminophores are connected through an sp^3-hybridized carbon atom, a spiro center, and are orthogonally arranged. These features lead to a reduction in crystallinity and an increase in T_g. As demonstrated by AFM measurements, high-quality amorphous films of spiro-**FPA** with good morphological stability can be prepared by vapor deposition. Multilayer organic EL devices constructed using spiro-**FPA** as an emitting layer produced bright blue emissions. With a 1.0-wt %-**TBP**-doped spiro-**FPA** emissive layer (20 nm), we achieved a high luminescence efficiency of 4.9 cd/A (2.07 lm/W) with CIE coordinates of $x = 0.134$ and $y = 0.207$ at a current density of 20 mA/cm^2 and a voltage of 7.4 V.

Acknowledgment. We thank the National Science Council of the Republic of China for financial support.

CM0345117